

# Impact of the Non-ideal Temperature Dependence of $I_C$ - $V_{BE}$ on Ultra-Wide Temperature Range SiGe HBT Bandgap Reference Circuits

Lan Luo, Guofu Niu, Laleh Najafizadeh<sup>1</sup>, and John D. Cressler<sup>1</sup>

ECE Department, 200 Broun Hall, Auburn University, Auburn, AL 36849, USA

<sup>1</sup> School of ECE, 777 Atlantic, Drive, N.W., Georgia Tech, Atlanta, GA 30332-0250, USA

**Abstract**— We investigate the impact of the non-ideal temperature dependence of  $I_C$ - $V_{BE}$  on the performance of ultra-wide temperature range SiGe HBT bandgap reference circuits. Both the slope and intercept of  $I_C$ - $V_{BE}$  show temperature dependences that significantly differ from “ideal” Shockley theory widely used in BGR analysis and design, and are shown to have significant impact on  $\Delta V_{BE}(T)$ ,  $I_C(T)$  and  $V_{BE}(T)$ .

**Keywords**—SiGe HBT, Bandgap reference, PTAT, Non-ideality factor, Saturation current

## I. INTRODUCTION

Due to its excellent analog and RF performance over an extremely wide range of temperatures [1], SiGe BiCMOS electronic components can operate robustly in the extreme temperature environments encountered in space exploration. Precision bandgap references (BGRs) are extensively used in a wide variety of circuits required for such missions, and have been demonstrated to work well at cryogenic temperatures [2] [3]. To further optimize BGR performance at cryogenic temperatures, it is necessary to understand and model the non-idealities found in existing designs, which we address in this work for the first time.

Typical BGR design assumes an ideal temperature dependence of the  $I_C$ - $V_{BE}$  characteristics predicted from Shockley’s transistor theory, with various degrees of assumptions on the temperature dependence of the bandgap. At cryogenic temperatures, however, the slope of measured  $I_C$ - $V_{BE}$  significantly deviates from ideal  $1/V_T$  [4] [5]. A temperature dependent non-ideality factor  $N_F(T)$  is necessary to describe the slope of  $I_C$ - $V_{BE}$ . The measured intercept of  $I_C$ - $V_{BE}$ , known as the saturation current  $I_S$ , also shows a temperature dependence drastically different from traditional theory below 200 K [4] [5]. It is therefore logical to examine how these device-level deviations from traditional theories affect BGR output at cryogenic temperatures. In addition, a key question centers of whether we can successfully model BGR performance over extremely-wide temperature ranges using the transistor  $I_C$ - $V_{BE}$  model of [5]. The first-order BGR design from [2] is used here, which was fabricated using a first-generation SiGe BiCMOS technology with 50 GHz cut-off frequency at room temperature.

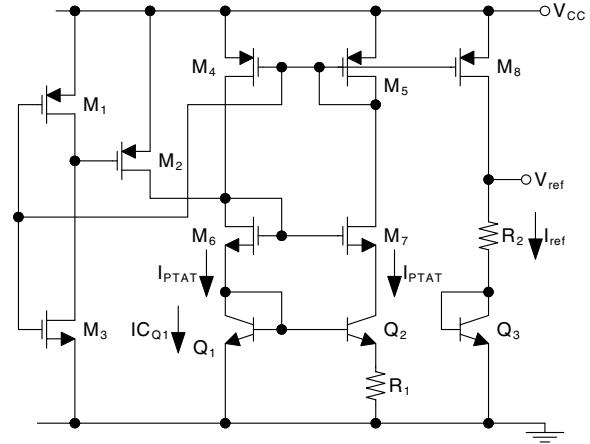


Fig. 1. Schematic of a first-order SiGe bandgap reference [2].

## II. TECHNICAL APPROACH AND RESULTS

Fig.1 shows the schematic of the BGR analyzed [2].  $M_4$ - $M_7$  and  $Q_1$ - $Q_2$ , along with resistor  $R_1$ , generate the PTAT bias current  $I_{PTAT}$ , which is set by  $\Delta V_{BE}$ .  $Q_1$  and  $Q_3$  consists of four parallel copies of  $0.5 \times 2.5 \mu\text{m}^2$  SiGe HBTs. The emitter area of  $Q_2$  is eight times of that of  $Q_1$  and  $Q_3$ .  $V_{BE}$  of  $Q_3$  is controlled by  $I_{PTAT}$ , and increases with cooling.  $V_{ref}$  is the sum of  $V_{BE}$  of  $Q_3$  and the voltage across  $R_2$ , PTAT voltage proportional to  $\Delta V_{BE}$  through  $I_{ref}(T)$ .

### A. Slope of $I_C$ - $V_{BE}$ and Impact on $\Delta V_{BE}(T)$ and $I_{ref}(T)$

The “PTAT”  $\Delta V_{BE}(T)$  is generated from the  $V_{BE}$  difference of  $Q_1$  and  $Q_2$ , two transistors operating at different current densities. Shockley theory predicts a  $I_C - V_{BE}$  slope of  $1/V_T$ , and a  $\Delta V_{BE}$  of  $V_T \ln \left( \frac{A_{Q2}}{A_{Q1}} \right)$ , which is  $V_T \ln(8)$ . However, the measured  $\Delta V_{BE}$  of the BGR clearly deviates from  $V_T \ln(8)$  below 200 K, which is shown in Fig. 2(a). This deviation from strict PTAT behavior originates from deviation of  $I_C - V_{BE}$  slope from  $1/V_T$ , and can be modeled using a non-ideality factor  $N_F(T)$  [5].  $\Delta V_{BE}(T)$  is then given by:

$$\Delta V_{BE}(T) = N_F(T) V_T \ln(8). \quad (1)$$

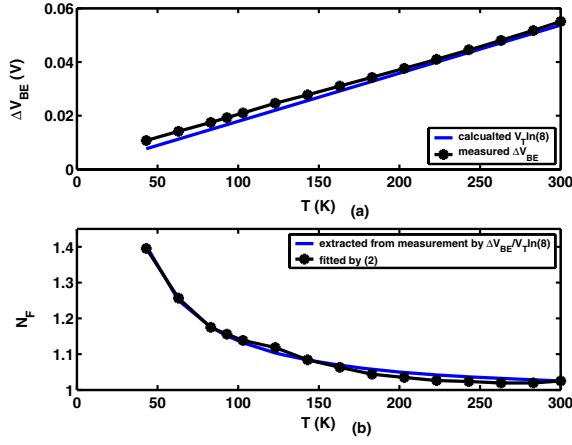


Fig. 2. (a) Measured  $\Delta V_{BE}$ - $T$  and calculated  $V_T \ln(8)$ - $T$  from 43 to 300 K. (b)  $N_F$ - $T$  from 43-300 K.

$N_F(T)$  can be modeled using [5]:

$$N_F(T) = N_{F,nom} \left( 1 - \frac{T - T_{nom}}{T_{nom}} \left( A_{NF} \frac{T_{nom}}{T} \right)^{X_{NF}} \right), \quad (2)$$

where  $T_{nom}$  is nominal temperature,  $N_{F,nom}$  is non-ideality factor at nominal temperature, which is close to unity, and  $A_{NF}$  and  $X_{NF}$  are technology dependent fitting parameters. Using (2),  $N_F(T)$  and consequently  $\Delta V_{BE}(T)$  can be well-modeled, as shown in Fig. 2(b).

Transistors  $M_4$ - $M_5$  and  $M_6$ - $M_7$  are identically-sized pairs.  $I_{PTAT}$  is then amplified through transistor  $M_8$ , with an amplification factor  $k = (W/L)_{M_8} / (W/L)_{M_5}$ .

$$I_{ref}(T) = k I_{PTAT}(T) = k \frac{N_F(T) V_T \ln(8)}{R_1}. \quad (3)$$

We mention in passing that the “PTAT” designation is no longer strictly accurate below 200 K because  $N_F(T) > 1$ . The slope of  $I_C$ - $V_{BE}$ , or  $1/N_F(T)V_T$ , directly affects the BGR’s  $\Delta V_{BE}(T)$  and hence  $I_{ref}(T)$ , which then determines  $V_{BE}$  of  $Q_3$ , as detailed below.

### B. $I_S(T)$ and Impact on $V_{BE}(T)$

$V_{BE}$  of  $Q_3$ ,  $V_{BE,3}$  is given by:

$$V_{BE,3} = N_F(T) V_T \ln \frac{I_{ref}(T)}{I_{S,3}(T)} = N_F(T) V_T \ln \frac{k \frac{\Delta V_{BE}(T)}{R_1}}{I_{S,3}(T)}, \quad (4)$$

where  $I_{S,3}$  is the  $I_S$  of  $Q_3$ .

We have seen that the slope of  $I_C - V_{BE}$  affects  $V_{BE,3}$  through the  $N_F(T)V_T$  term. The intercept of  $I_C$ - $V_{BE}$ ,  $I_S(T)$ , further affects  $V_{BE,3}$  through the  $I_{S,3}(T)$  term in (4).

The most complete  $I_S(T)$  expression derived using ideal Shockley transistor theory was given by Tsividis [6]. Using the popular nonlinear bandgap-temperature relation  $E_{g,t} = E_{g,0} - \alpha T^2 / (T + \beta)$  [7], the result can be rewritten in a form

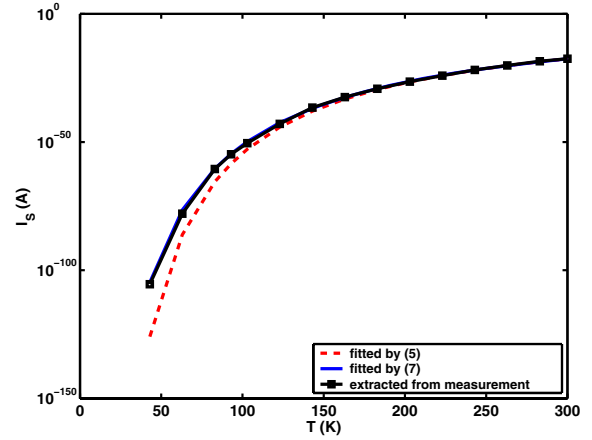


Fig. 3.  $I_S$  extracted from measurement vs.  $I_S$  fitted by (5) and (7) for single  $0.5 \times 2.5 \mu m^2$  SiGe HBT from 43-300 K.

that resembles the  $I_S(T)$  equations found in compact models:

$$I_S(T) = I_{S,nom} \left( \frac{T}{T_{nom}} \right)^{X_{IS}} \exp \left( \frac{-E_{a,t} \left( 1 - \frac{T}{T_{nom}} \right)}{V_T} \right), \quad (5)$$

$$E_{a,t} = E_{a,nom} - \frac{\alpha \beta T_{nom}^2}{(T_{nom} + \beta)^2} + \frac{\alpha \beta T T_{nom}}{(T + \beta)(T_{nom} + \beta)}, \quad (6)$$

where  $E_{a,t}$  appears in the place of bandgap activation energy  $E_A$  in VBIC (other compact models use different symbols), but is now temperature dependent due to the nonlinear temperature dependence of  $E_{g,t}$ .  $E_{a,nom}$  is the extrapolated 0 K  $E_g$  at nominal temperature, usually 300 K, and  $I_{S,nom}$  is  $I_S$  at nominal temperature.  $X_{IS}$  includes the temperature coefficient of mobility and density of states,  $\alpha = 4.45 \times 10^{-4}$  V/K,  $\beta = 686$  K, and  $E_{a,nom}$ ,  $I_{S,nom}$ , and  $X_{IS}$  are model parameters.

We observe that the measured  $I_S(T)$  is much higher than prediction of (5), by orders of magnitudes at lower temperatures, as shown in Fig. 3. Even though the underlying physics is not yet understood, the measured  $I_S(T)$  - $T$  can be well modeled by [5]:

$$I_S(T) = I_{S,nom} \left( \frac{T}{T_{nom}} \right)^{\frac{X_{IS}}{N_F(T)}} \exp \left( \frac{-E_{a,t} \left( 1 - \frac{T}{T_{nom}} \right)}{N_F(T) V_T} \right). \quad (7)$$

The effectiveness of (7) in modeling  $I_S(T)$  can be seen in Fig. 3.

We now examine the impact of  $I_S(T)$  on  $V_{BE,3}$ . To examine the roles of the  $I_C - V_{BE}$  slope and intercept, that is,  $N_F(T)$  and  $I_S(T)$ , we chose 3 model combinations, as shown in Table 1. Model 1 produces the classic slope and intercept models, both of which are “wrong” at lower temperatures. Model 2 produces the correct slope but the “wrong” intercept. Model 3 produces the correct slope and the correct intercept of  $I_C$ - $V_{BE}$ .

TABLE I  
MODELS EXAMINED IN THIS WORK.

Name	Model 1	Model 2	Model 3
$N_F(T)$	1.025	(2)	(2)
$I_S(T)$	(5)	(5)	(7)

Fig. 4 shows  $I_C$ - $V_{BE}$  for a  $0.5 \times 2.5 \mu m^2$  SiGe HBT at 300 K and 43 K. The symbols represent the  $(V_{BE,3}, I_{ref}/4)$  pair using (3) and (4). The factor of “4” represents the multiplicity number of  $Q_3$ . At 300 K, the nominal temperature, all of the three models have the same  $I_{ref}$  value, and give the same  $V_{BE,3}$ , because they all have the same  $N_F$  and  $I_S$  at 300 K, as expected.

At 43 K, with  $N_F(T)$ , the slope of  $I_C - V_{BE}$  is correctly modeled by both model 2 and model 3. Model 2 and 3 thus have the same and correct  $I_{ref}$ . However, for model 2,  $I_S$  is underestimated by traditional theory, leading to a much higher  $V_{BE,3}$  than model 3.

For model 1, the situation is more complex. The slope of  $I_C - V_{BE}$  is overestimated as  $N_F$  is fixed at its 300 K value. The intercept of  $I_C - V_{BE}$  ( $I_S$ ) is underestimated. The final  $I_C - V_{BE}$  from a model that gives a wrong slope and a wrong intercept, however, is surprisingly not too far off from measured data in the current range of interest for producing  $V_{BE,3}$ . As a result, the  $V_{BE,3}$  from model 1, the traditional model, is much closer to model 3 than model 2, which actually has the correct slope.

The above process can be repeated for all temperatures to yield  $V_{BE,3}$ - $T$ , which is shown in Fig. 5. This is completely equivalent to a calculation using (4), but the graphical illustration yields a much better intuitive understanding of the model differences. Model 3 successfully reproduces the measured  $V_{BE,3}$ - $T$  characteristics. The  $V_{BE,3}$ - $T$  prediction from traditional theory, model 1, is not terribly inaccurate, because of the cancellation between underestimated intercept,  $I_S(T)$ , and the overestimated slope,  $1/N_F(T)V_T$ . This cancellation is circuit design dependent, however, and is to a large extent a coincidence for the BGR design analyzed.

### C. $V_{ref}(T)$

The BGR output  $V_{ref}$  is given by:

$$V_{ref}(T) = V_{BE,3}(T) + I_{ref}(T)R_2 = V_{BE,3}(T) + K\Delta V_{BE}(T), \quad (8)$$

where  $K = kR_2/R_1$ . The temperature dependence of  $K$  can be negligibly small by choosing high precision, low temperature coefficient resistors and careful layout design to minimize resistor mismatch. The resistor used in the BGR exhibits a temperature coefficient of 17.8 ppm/ $^\circ C$  over the temperature range of 43-300 K. In practice,  $K$  is often chosen to make the positive temperature coefficient of  $\Delta V_{BE}(T)$  cancel the negative temperature coefficient of  $V_{BE}(T)$ , to produce a zero temperature coefficient  $V_{ref}(T)$  at a nominal temperature, usually 300 K [6] [8].

Fig. 6 shows the measured and modeled  $K \times \Delta V_{BE}$  versus

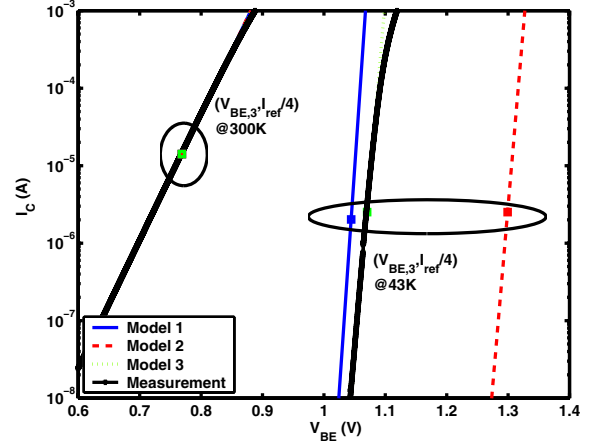


Fig. 4. Measured and modeled  $I_C$ - $V_{BE}$  for single  $0.5 \times 2.5 \mu m^2$  SiGe HBT at 43 K and 300 K.

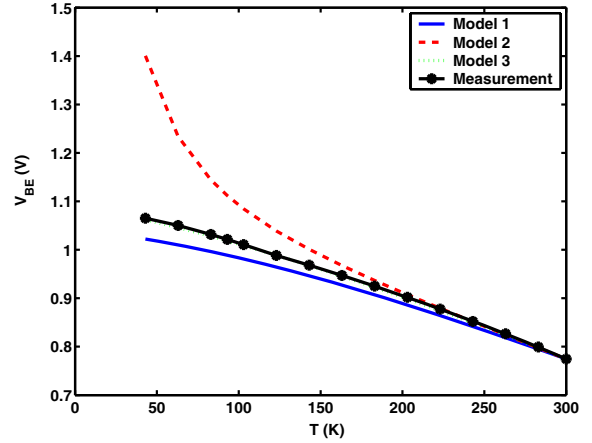


Fig. 5. Measured and modeled  $V_{BE}$  from 43-300 K.

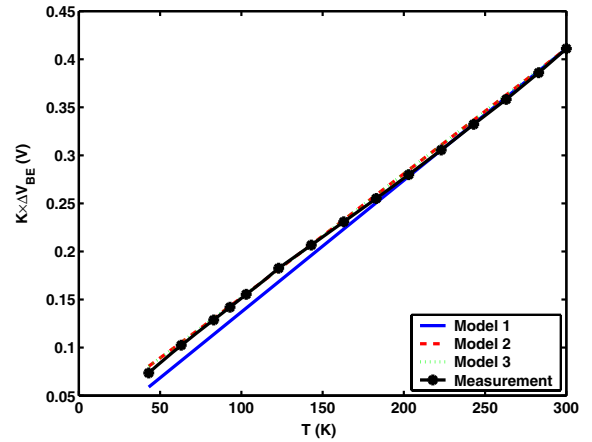


Fig. 6. Measured and modeled  $K \times \Delta V_{BE}$  from 43-300 K.

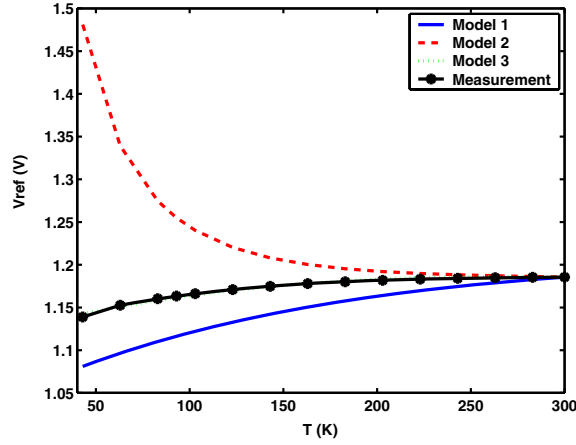


Fig. 7. Measured and modeled  $V_{ref}$  from 43-300 K.

temperature. Due to the use of a constant  $N_F$ , model 1 deviates from measurements below 200 K. Model 2 and 3 accurately capture  $K \times \Delta V_{BE}$ .

The sum of  $V_{BE,3}(T)$  and  $K \times \Delta V_{BE}(T)$  gives  $V_{ref}$ , which is shown in Fig. 7. Additional calculation shows that the  $V_{BE,3}(T)$  difference between the models dominates over the  $K \times \Delta V_{BE}$  differences. Model 2 has the largest  $V_{BE,3}$  and hence  $V_{ref}$  deviation from measurement. Traditional theory, model 1, is not terrible in predicting  $V_{ref}$ , because of coincidental cancellation between underestimated intercept,  $I_S(T)$ , and overestimated slope,  $1/N_F(T)V_T$ .

On the other hand, we observe that the overall  $V_{ref}$  variation with temperature for model 3 is less than that for model 1. The difference is that model 3 accounts for the deviations of both the slope and intercept of  $I_C - V_{BE}$  from traditional Shockley transistor theory, model 1. This suggests that such deviations actually help make the BGR output vary less with temperature than traditional theories would predict, and explains why BGRs experimentally perform much better than predictions using traditional BGR design equations at lower temperatures.

### III. SUMMARY

We have examined the impact of the non-ideal temperature dependence of  $I_C - V_{BE}$  in SiGe HBTs across temperature on the output of a first-order SiGe bandgap reference. These nonidealities are shown to actually help make the BGR output voltage vary less at cryogenic temperatures than traditional Shockley theory would predict. For the particular BGR design examined, the overall  $V_{ref}(T)$  prediction from Shockley theory is not too bad, because of the cancellation between underestimated intercept and overestimated slope. Successful cryogenic temperature modeling of both  $\Delta V_{BE}$  and  $V_{BE}$  components of the BGR output is demonstrated for the first time. The modeling method presented provides basis for further optimization of SiGe BGRs operating across extremely wide temperature ranges, and down to deep cryogenic temperatures, where existing design equations fail.

### ACKNOWLEDGMENTS

This work was supported by NASA ETDP under grant NNL06AA29C. We are grateful for the support of A. Keys, D. Hope, M. Beatty, and S. Johnson of NASA; E. Kolawa of JPL, and the IBM SiGe development group, as well as the many contributions of the SiGe ETDP team, including: H. Mantooth, M. Mojarradi, B. Blalock, W. Johnson, R. Garbos, R. Berger, F. Dai, L. Peltz, J. Holmes, P. McCluskey, M. Alles, R. Reed, and C. Eckert.

### REFERENCES

- [1] J. D. Cressler, "On the potential of SiGe HBTs for extreme environment electronics," in *Proceedings of the IEEE*, vol. 93, pp. 1559–1582, Sep 2005.
- [2] L. Najafizadeh, A. K. Sutton, R. M. Diestelhorst, M. Bellini, B. Jun, J. D. Cressler, P. W. Marshall, and C. J. Marshall, "A comparison of the effects of X-Ray and proton irradiation on the performance of SiGe precision voltage references," *IEEE Transactions on Nuclear Science*, vol. 54, pp. 2238–2244, Dec 2007.
- [3] L. Najafizadeh, J. S. Adams, S. D. Phillips, K. A. Moen, J. D. Cressler, T. R. Stevenson, and R. M. Meloy, "Sub-1-K operation of SiGe transistors and circuits," *IEEE Electron Device Letters*, vol. 30, pp. 508–510, May 2009.
- [4] Z. Feng, G. Niu, C. Zhu, L. Najafizadeh, and J. D. Cressler, "Temperature scalable modeling of SiGe HBT DC current down to 43 K," in *ECS Trans.*, vol. 3.
- [5] Z. Xu, X. Wei, G. Niu, L. Luo, D. Thomas, and J. D. Cressler, "Modeling of temperature dependent  $I_C - V_{BE}$  characteristics of SiGe HBTs from 43–400K," in *Dig. of IEEE BCTM*, pp. 81–84, oct 2008.
- [6] Y. P. Tsividis, "Accurate analysis of temperature effects in  $I_C - V_{BE}$  characteristics with application to bandgap reference sources," *IEEE Journal of Solid-State Circuits*, vol. 15, pp. 1076–1084, Dec 1980.
- [7] C. D. Thurmond, "The standard thermodynamic functions for the formation of electrons and holes in Ge, Si, GaAs, and GaP," *Journal of Electrochemical Society*, vol. 122.
- [8] P. R. Gray and R. G. Meyer, eds., *Analysis and Design of Analog Integrated Circuits*. New York: Wiley, 2001.